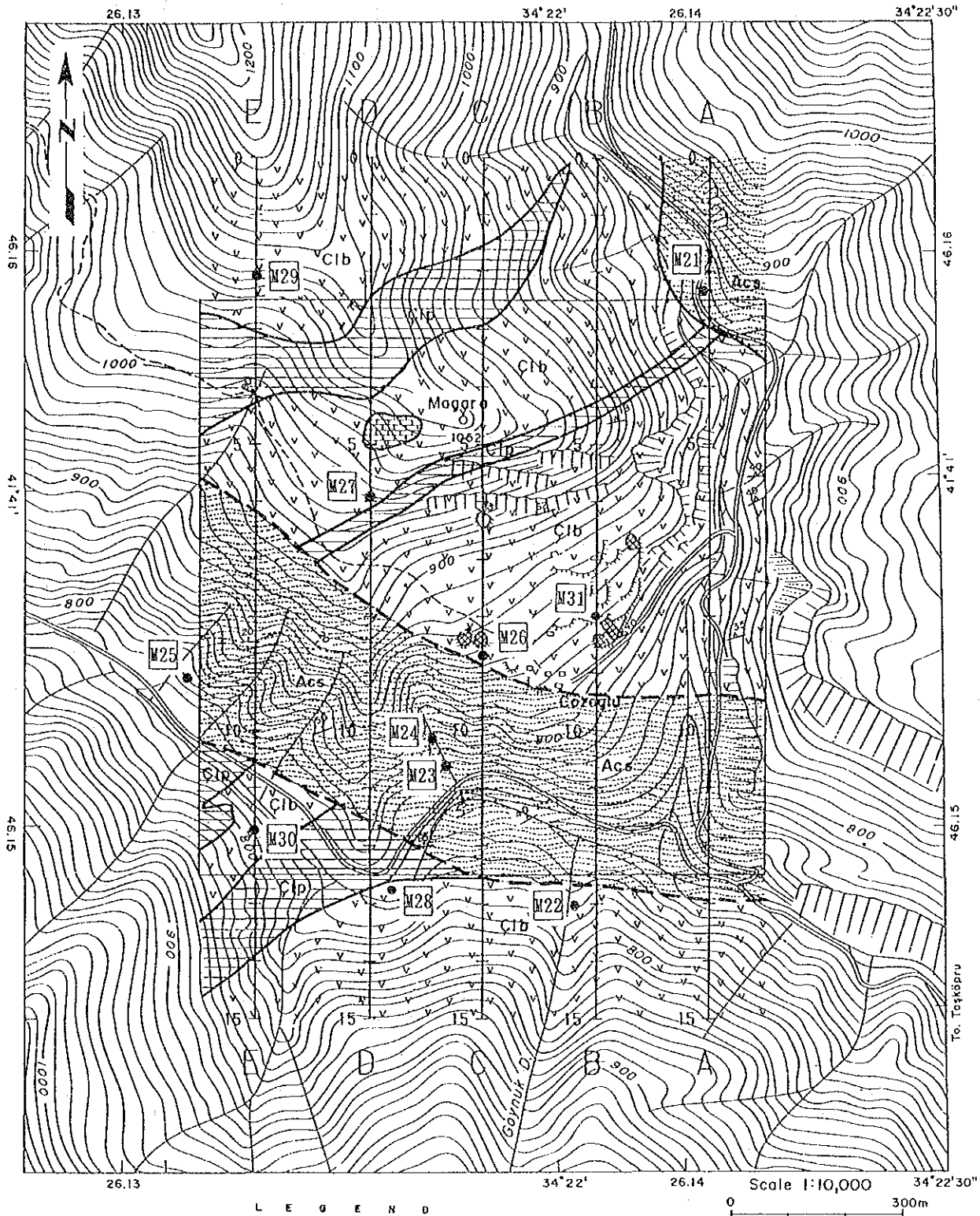


small houses and a telephone line along the road and the possibility of electromagnetic coupling is very limited. Thus, it is believed that the negative anomalies occur from geologic conditions. The laboratory work show the resistivity of the sandstone and shale samples of this area lies within the range of 890-1740ohm-m and is higher than similar rocks of other areas. These rocks are compact and this could be caused by ionic solution filling the interstices of fragmented rocks.



L E G E N D

Aloçam Formation	Acs	Sandstone and shale	---	Fault
Kızocak Formation	Kcl	Limestone	20	Strike and dip of strata
Çoçulu Metaophyllite	Cib	Metabasalt and green schist	60	Strike and dip of schistosity
	Cjp	Pelitic schist		
Mineralization and alteration	[Symbol]	Gossan with quartz vein	● M25	Location and number of sample for ore assay
	[Symbol]	Slag		
	[Symbol]	Adit		
	[Symbol]	Dump		

Fig. 3-11 Location Map of IP Survey Lines in the Cozoglu Prospect

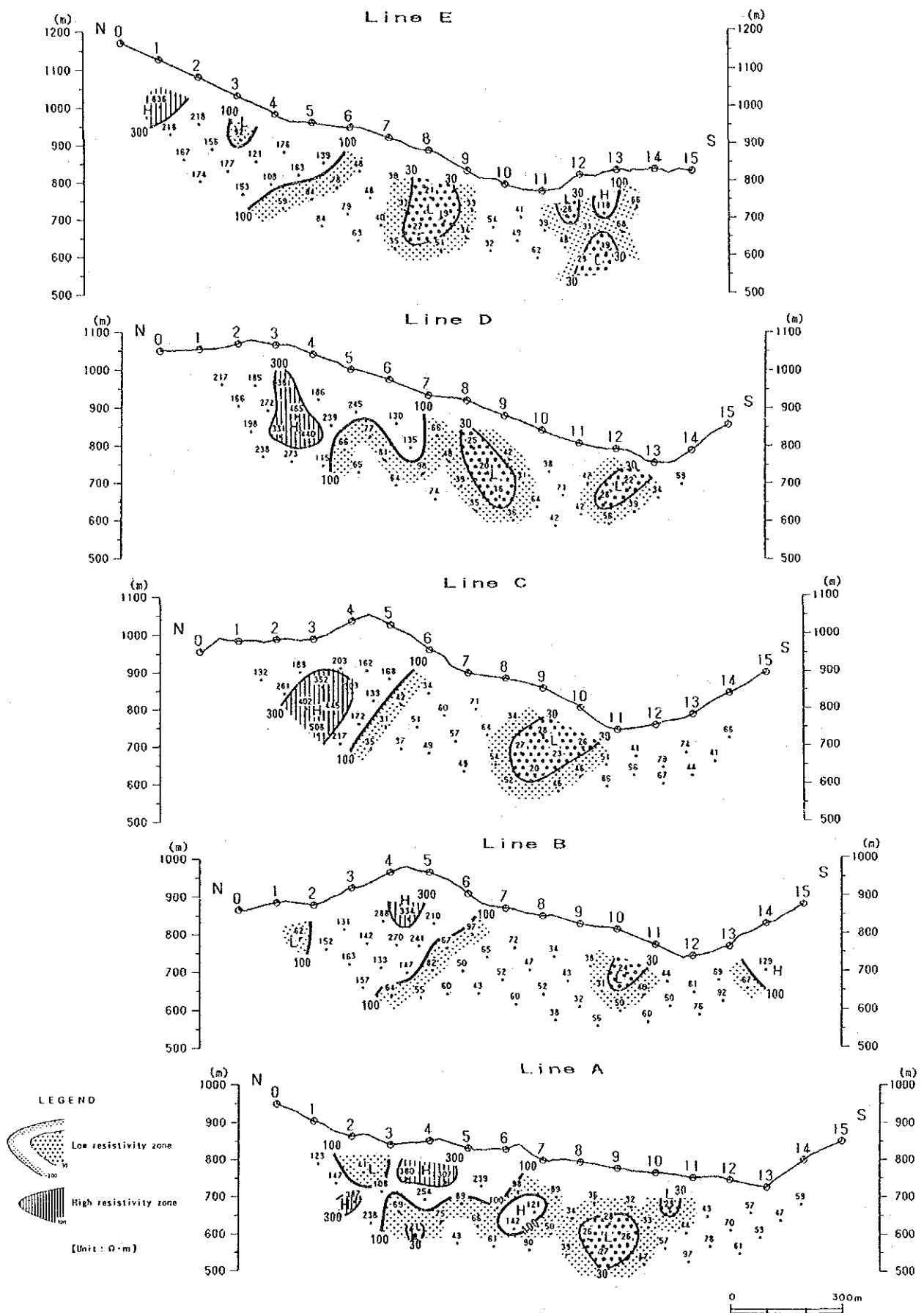
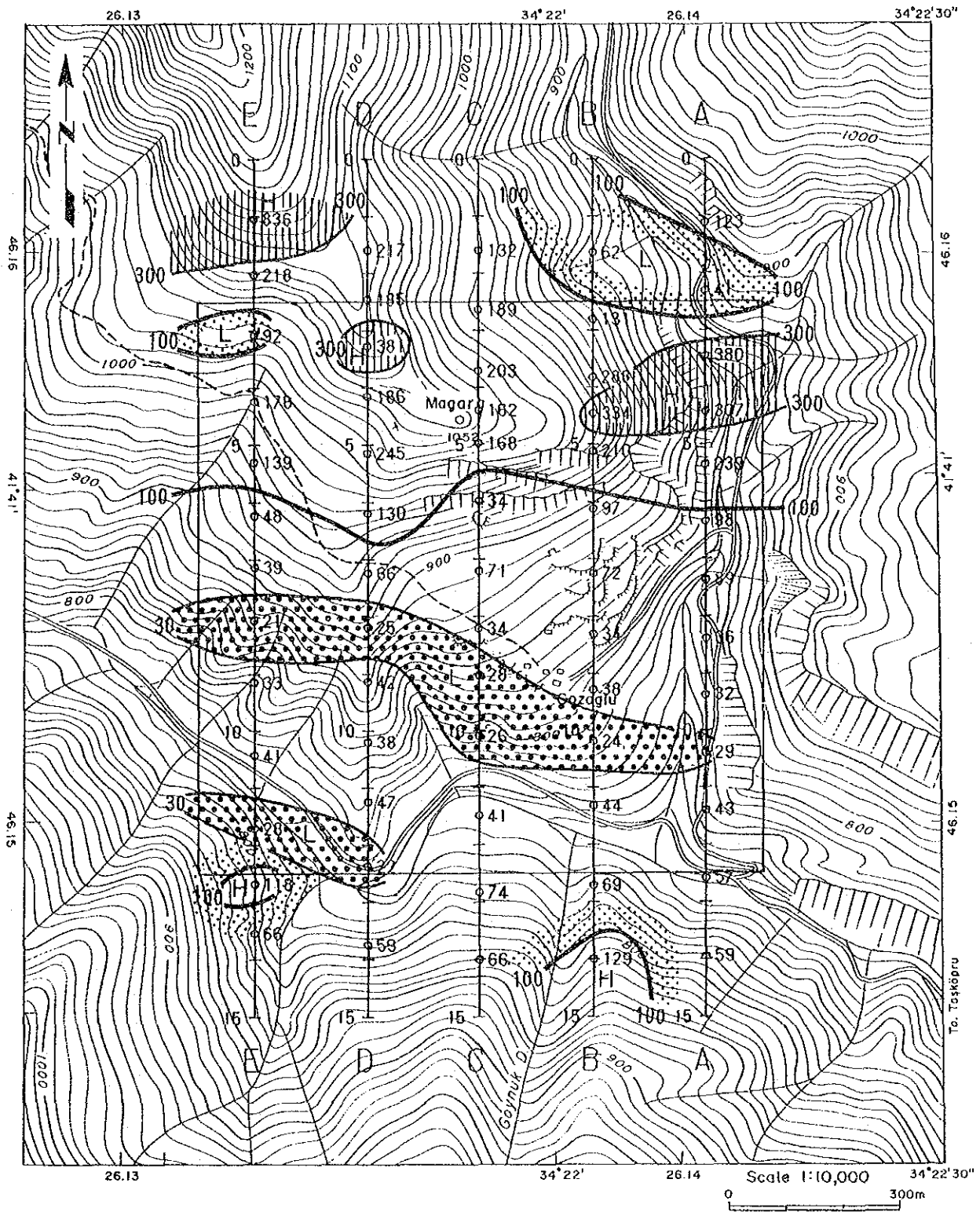
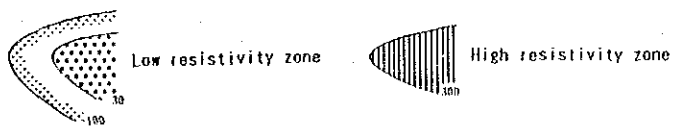


Fig.3-12 Sections of Apparent Resistivity (Line A ~ E)

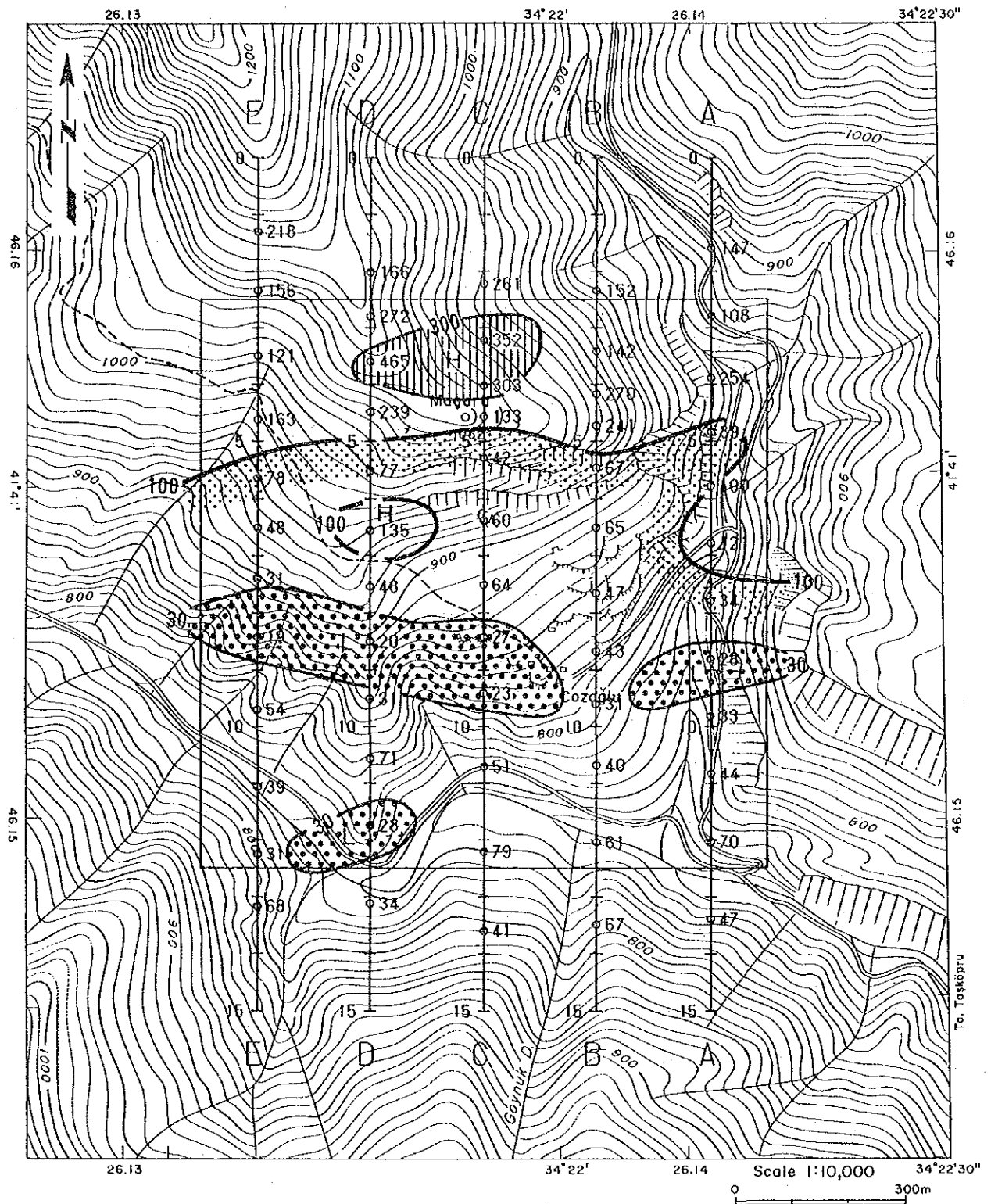


LEGEND

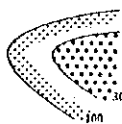


[Unit : 0·m]

Fig.3-13-1 Plan Map of Apparent Resistivity (n=1, -100m)



LEGEND



Low resistivity zone



High resistivity zone

[Unit: $\Omega \cdot m$]

Fig. 3-13-2 Plan Map of Apparent Resistivity (n=2, -150m)

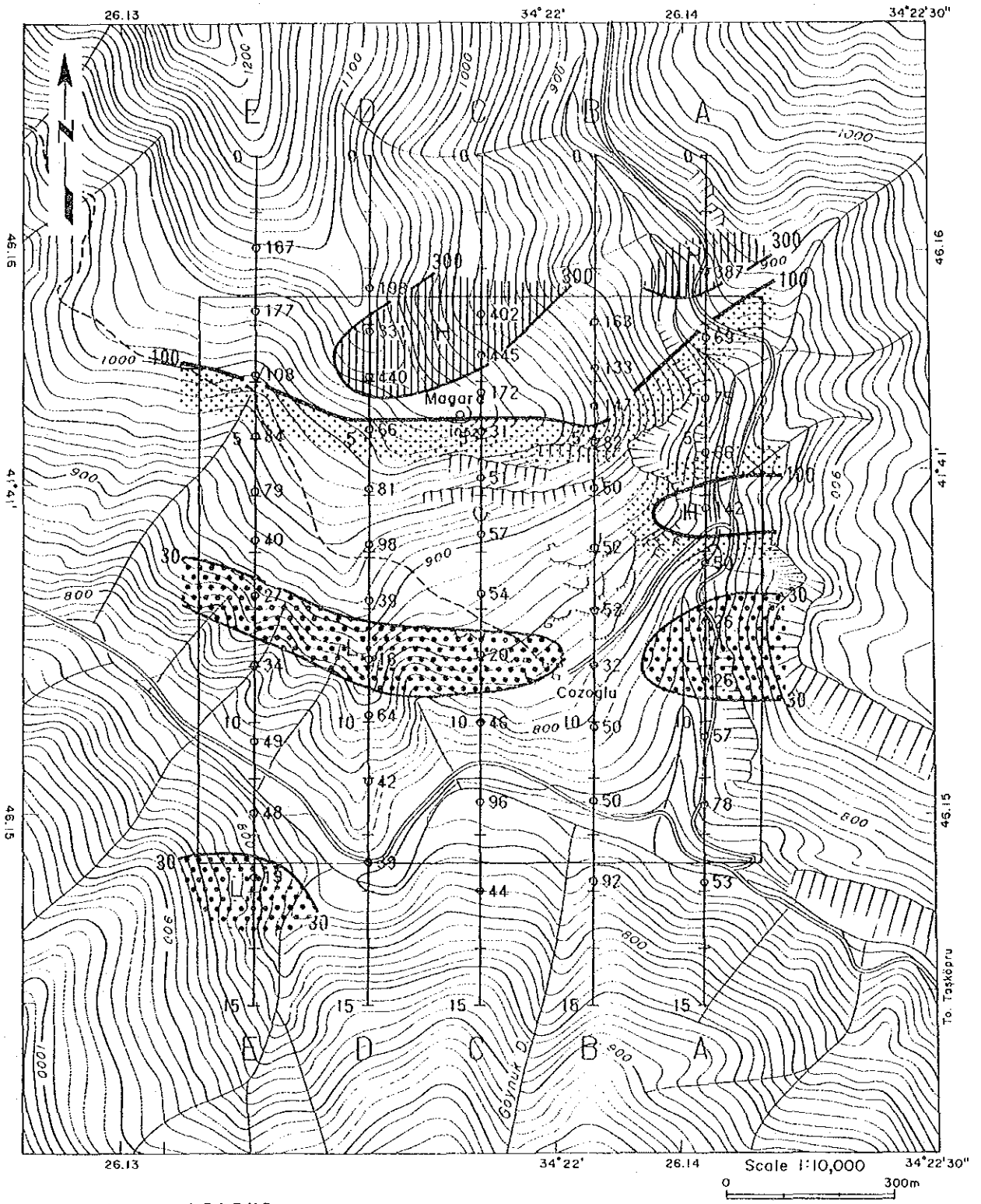


Fig. 3-13-3 Plan Map of Apparent Resistivity (n=3, -200m)

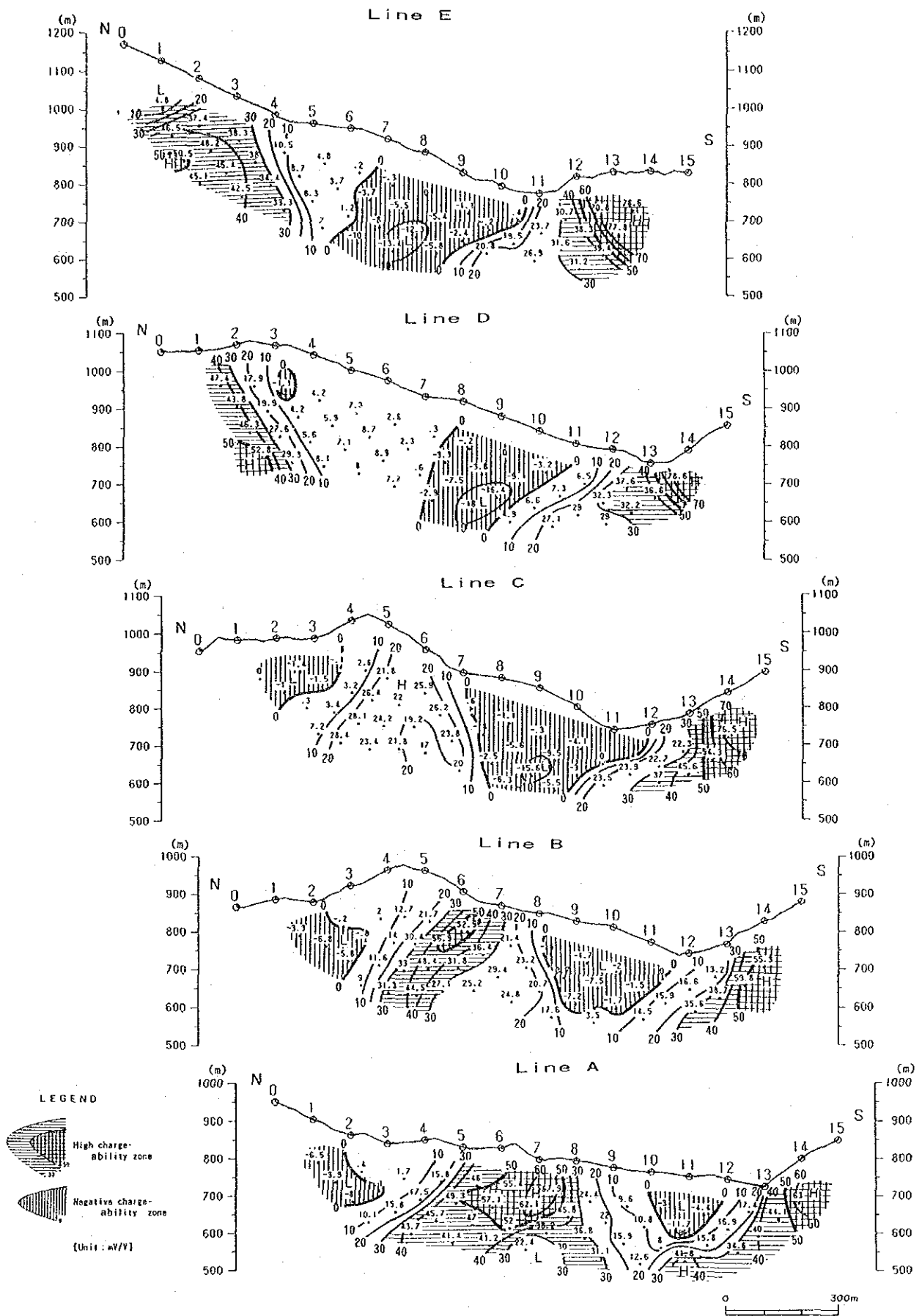
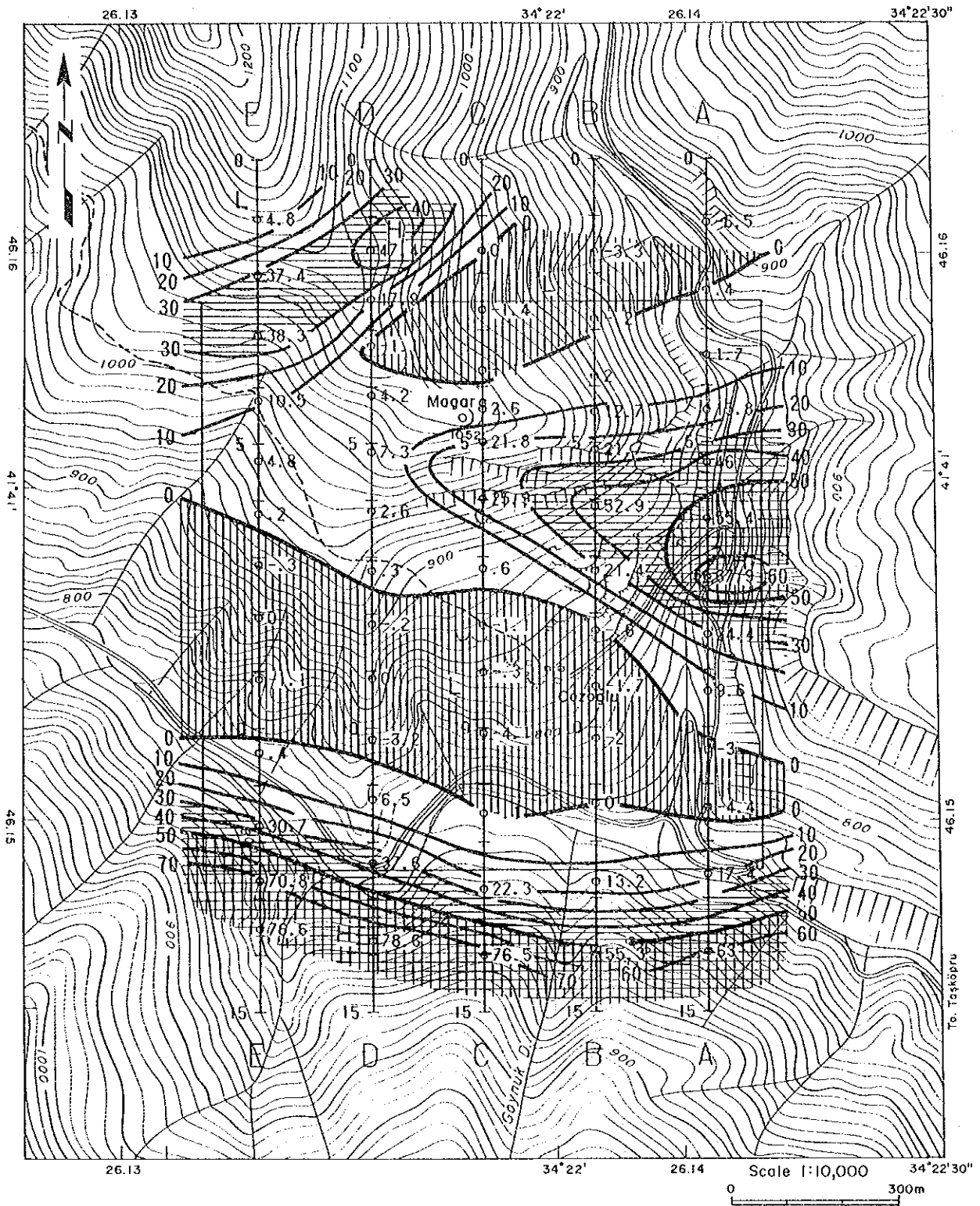
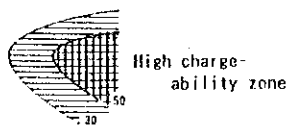


Fig. 3-14 Sections of Chargeability (Line A - E)



LEGEND



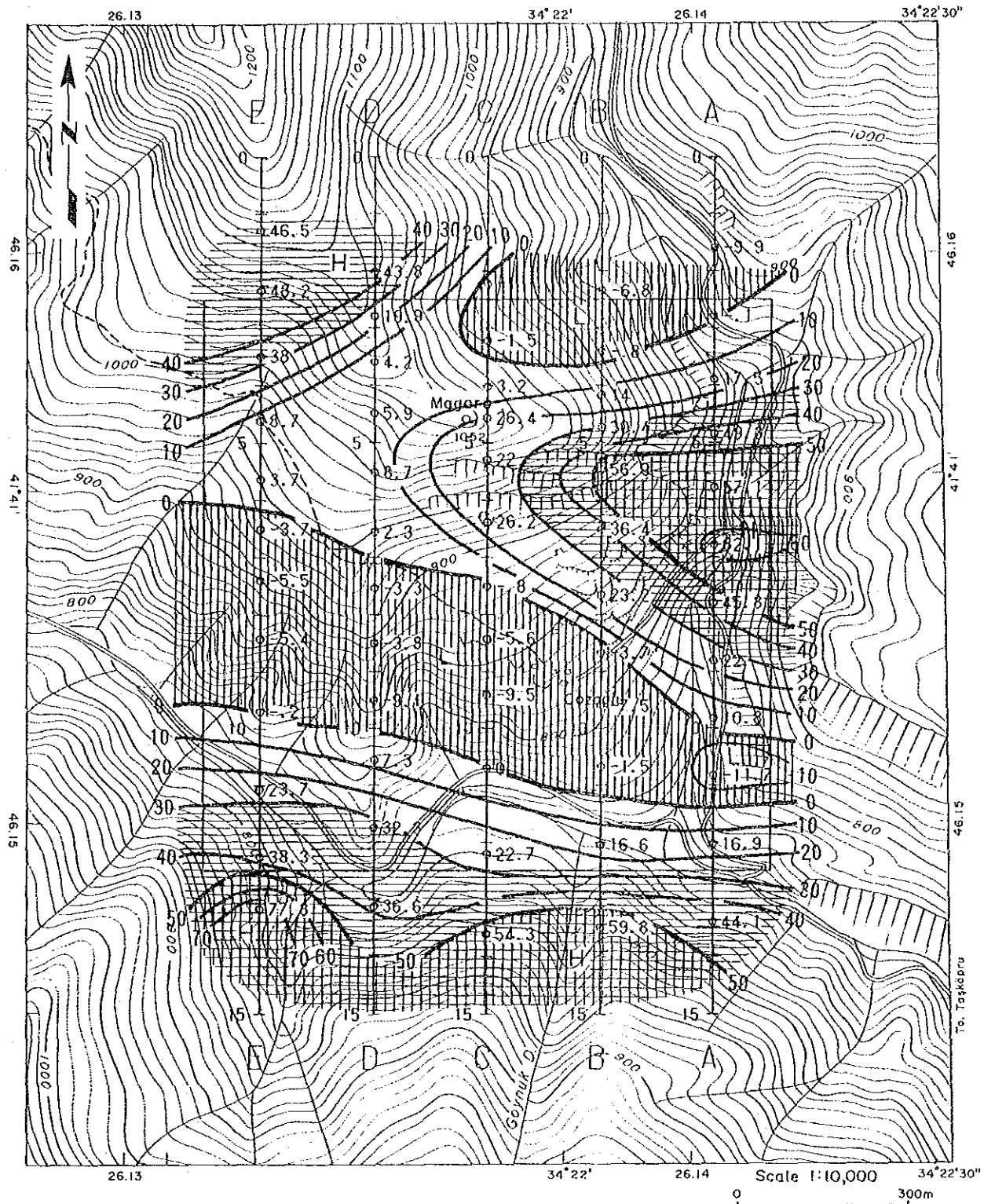
High charge-ability zone



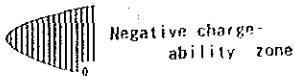
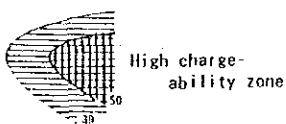
Negative charge-ability zone

[Unit: mV/V]

Fig.3-15-1 Plan Map of Chargeability (n=1, -100m)

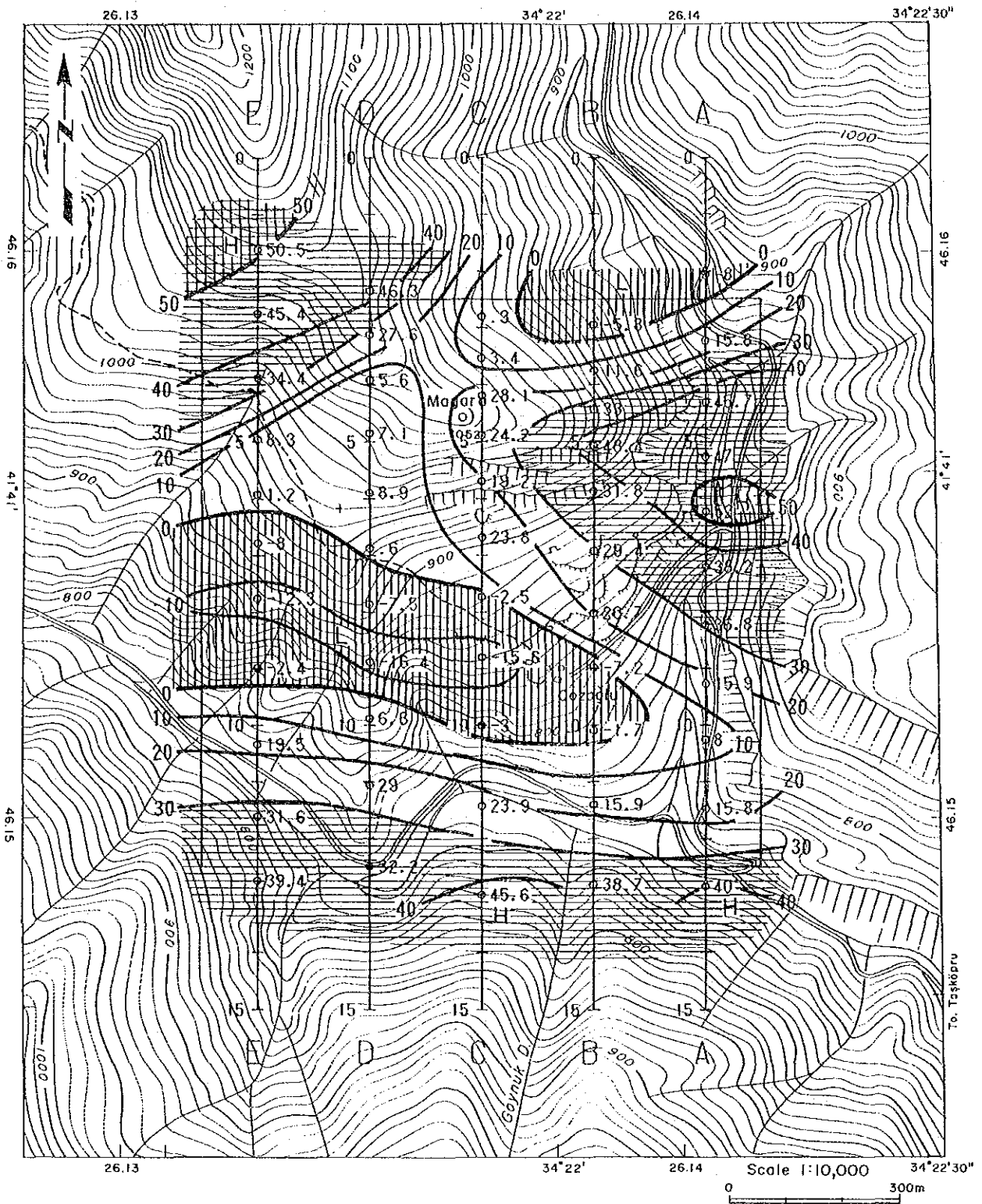


LEGEND



[Unit: mV/V]

Fig. 3-15-2 Plan Map of Chargeability (n=2, -150m)

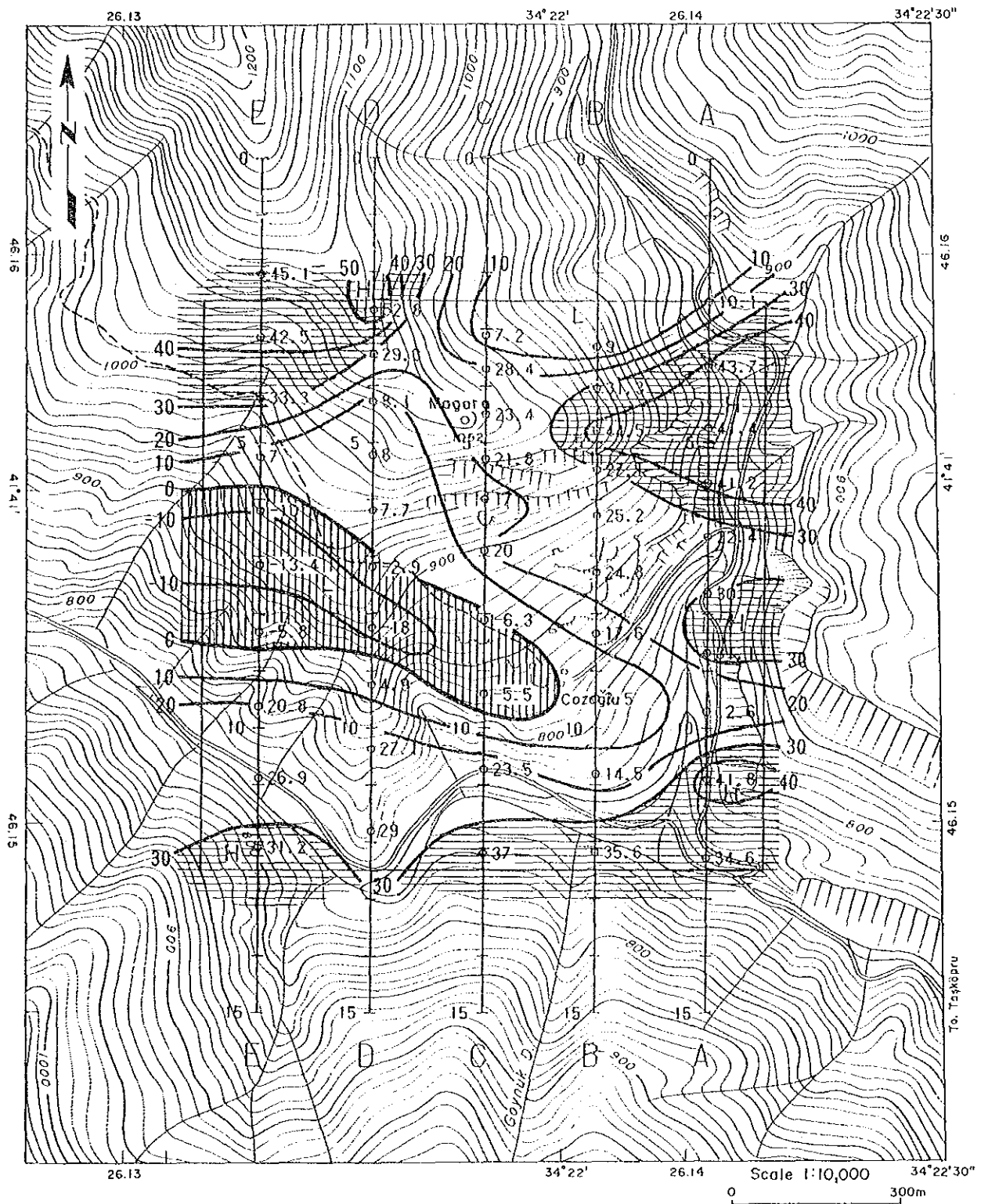


LEGEND

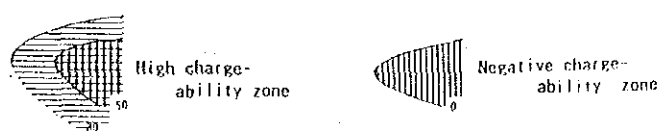


[Unit: mV/V]

Fig.3-15-3 Plan Map of Chargeability (n=3, -200m)

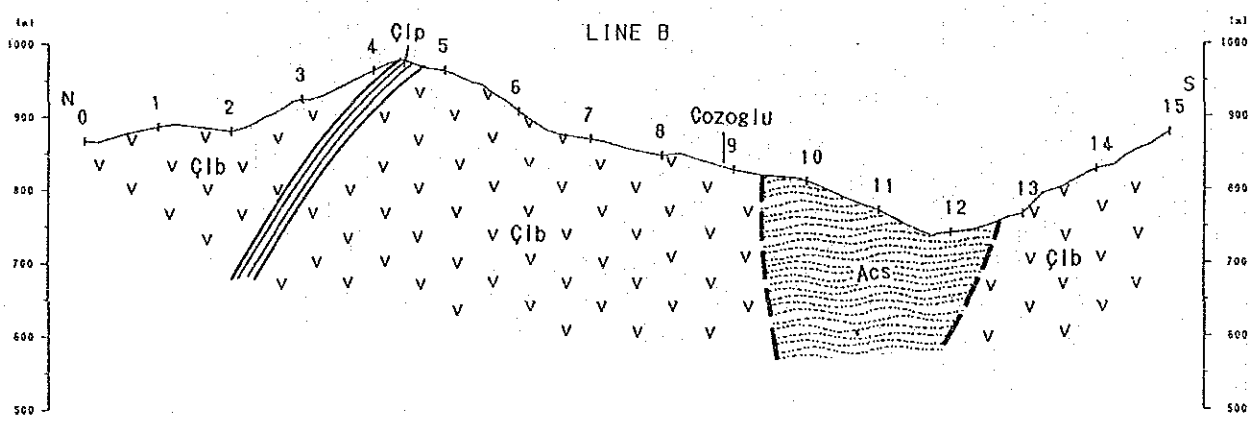
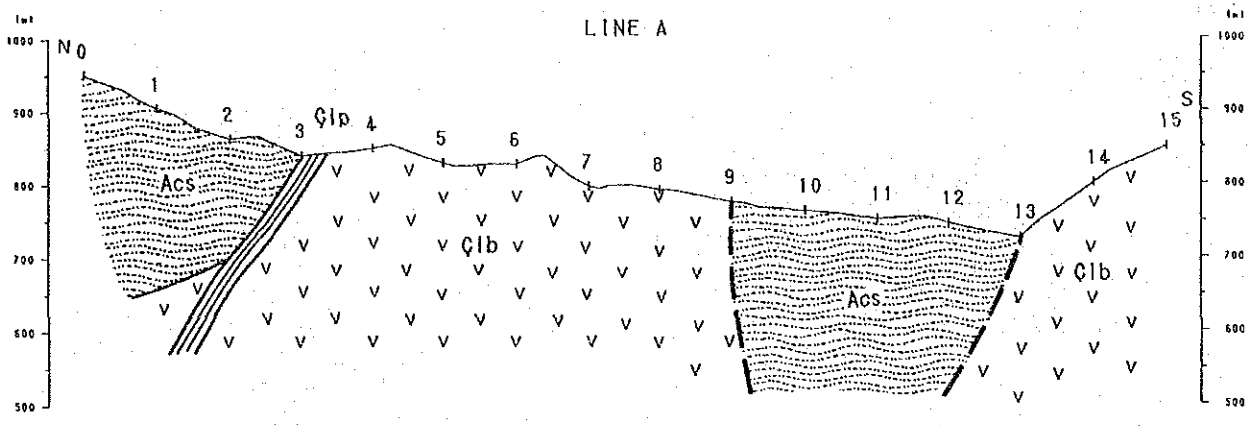


LEGEND

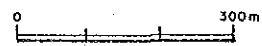


[Unit : mV/V]

Fig. 3-15-4 Plan Map of Chargeability (n=4, -250m)



Scale 1:10,000



L E G E N D

- | | | | |
|---------------------|--|-----|-----------------------------|
| Açoç Formation | | ACS | Sandstone and shale |
| Çangol Metaphyllite | | Çib | Metabasalt and green schist |
| | | | Çip |
| | | | Fault |

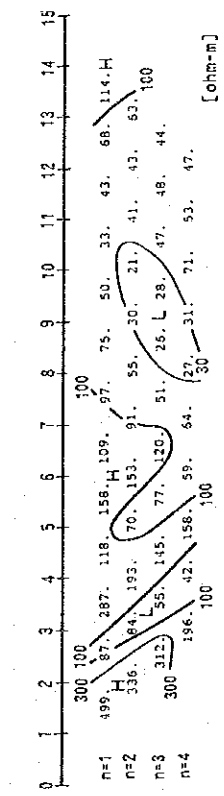
Fig. 3-16 Geological Sections of IP Survey Lines A & B in the Cozoglu Prospect

Simulation Model Line A

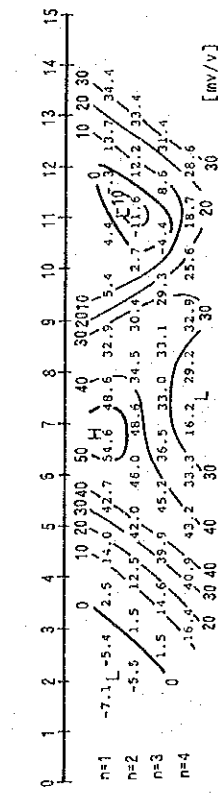
CODE	RESISTIVITY Ohm-m	CHARGEABILITY mV/V
1	100	10.0
2	50	-5.0
3	20	-3.0
4	20	10.0
5	100	50.0
6	300	10.0
7	300	-5.0
8	0	0
9	0	0

0	1	2	3	4	5	6	7	8	9	10	11	12	13	14	15
1	777	222	777	711	666	655	555	511	111	111	111	111	111	155	555
2	777	777	777	711	666	655	555	511	111	344	444	111	155	555	555
3	777	777	777	711	111	155	555	511	444	444	444	111	155	555	555
4	777	777	777	711	111	155	555	511	444	444	444	111	111	155	555
5	777	777	777	711	111	155	555	511	444	444	444	111	111	155	555
6	777	777	777	711	111	155	555	511	444	444	444	111	111	155	555
7	777	777	111	111	111	155	555	511	444	444	444	111	111	155	555
8	777	777	111	111	111	155	555	511	444	444	444	111	111	155	555
9	777	777	111	111	111	155	555	511	444	444	444	111	111	155	555
10	777	777	111	111	111	155	555	511	444	444	444	111	111	155	555
11	777	777	111	111	111	155	555	511	444	444	444	111	111	155	555
12	777	777	111	111	111	155	555	511	444	444	444	111	111	155	555
13	777	777	111	111	111	155	555	511	444	444	444	111	111	155	555
14	777	777	111	111	111	155	555	511	444	444	444	111	111	155	555
15	777	777	111	111	111	155	555	511	444	444	444	111	111	155	555
16	777	777	111	111	111	155	555	511	444	444	444	111	111	155	555

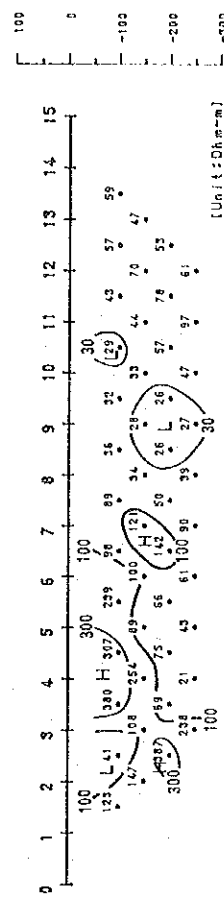
APPARENT RESISTIVITY



CHARGEABILITY



APPARENT RESISTIVITY (OBSERVED)



CHARGEABILITY (OBSERVED)

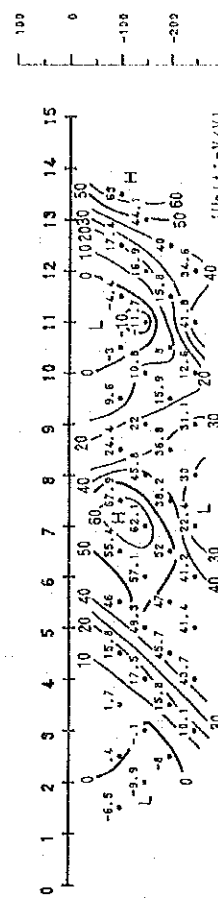


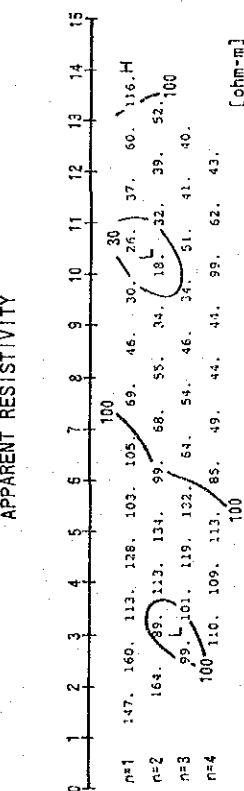
Fig. 3-17-1 Results of Two-dimensional Model Simulation (Line A)

Simulation Model Line B

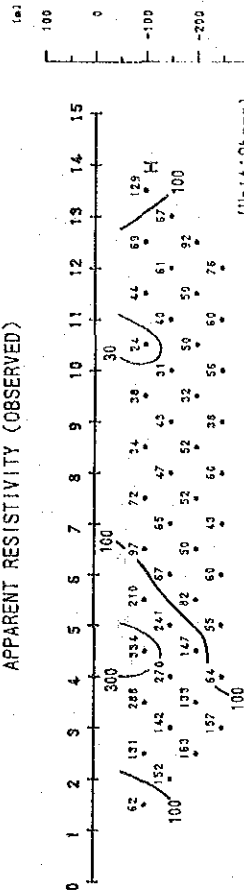
CODE	RESISTIVITY Ohm-m	CHARGEABILITY mV/V
1	677	776
2	677	677
3	666	666
4	666	666
5	666	666
6	666	666
7	666	666
8	666	666
9	666	666
10	666	666
11	666	666
12	666	666
13	666	666
14	666	666
15	666	666
16	666	666

CODE	RESISTIVITY Ohm-m	CHARGEABILITY mV/V
1	155	555
2	155	555
3	155	555
4	155	555
5	155	555
6	155	555
7	155	555
8	155	555
9	155	555
10	155	555
11	155	555
12	155	555
13	155	555
14	155	555
15	155	555
16	155	555

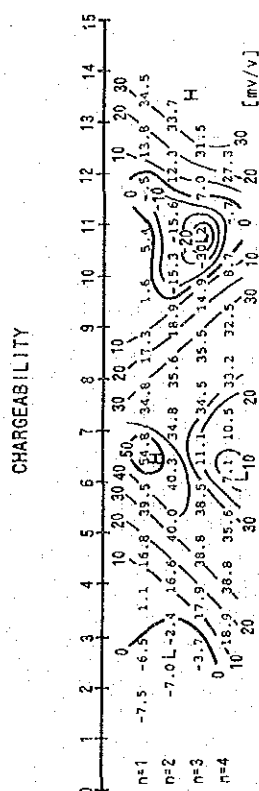
APPARENT RESISTIVITY



APPARENT RESISTIVITY (OBSERVED)



CHARGEABILITY



CHARGEABILITY (OBSERVED)

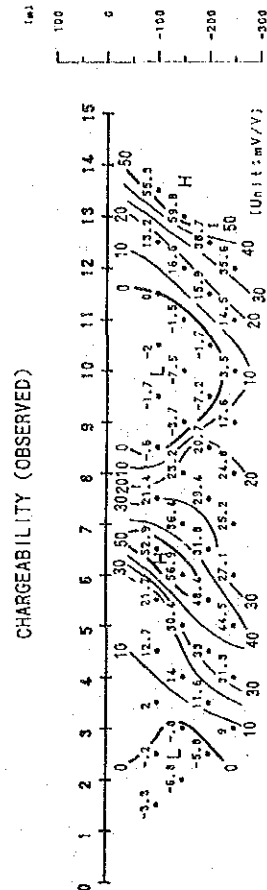


Fig. 3-17-2 Results of Two-dimensional Model Simulation (Line B)

**PART 4 CONCLUSIONS AND
RECOMMENDATIONS**

PART 4. CONCLUSIONS AND RECOMMENDATIONS

CHAPTER 1 CONCLUSIONS

1-1 Küre Zone

(1) The geology of the zone consists of pre-Jurassic ultramafic rocks, Jurassic basalt, sedimentary rocks of the Küre Formation, grayish white fossiliferous limestone of the Lower Cretaceous Karadana Formation, pale brown and white marl of the Upper Cretaceous Çağlayan Formation, talus deposits and intrusive diorite and dacite.

(2) The major part of the zone is occupied by the Jurassic Küre Formation. The basalt is composed of pillow lava, hyaloclastite, and massive basalt. Sedimentary facies of the Küre Formation is composed of angularly fragmentated graywacke and tectonically sheared/argillized black shale. The matrix consists of pelitic materials.

Basalt and brecciated sediments of the Küre Formation are interpreted as a constituent of mélangé. The period of mélangé formation is inferred to be Middle Jurassic, since intrusion into the mélangé is inferred to be Later Dogger epoch.

(3) The geologic structure of this zone is characterized by many faults. They are divided into two systems; N-S and E-W. The former system is crosscut by the latter. With the exception of the diorite and dacite intrusive bodies and the Karadana Formation, the boundaries of all geologic units, including ultramafic bodies, have been dislocated. The surface elongation of the intrusive bodies is harmonious with the strike of the faults in the vicinity and with the boundary between sediments and basalt of the Küre Formation.

Basalt is interpreted to be footwall rocks of ore deposits. It is distributed extending to N-S and NNW-SSE direction with imbricate structure.

(4) The known ore deposits are the Cyprus-type deposits. The new ore deposits of the same type are expected to occur in the zone. They occur at the boundary between hyaloclastite and black shale of the Küre Formation and also within hyaloclastite. They consist of massive ore, brecciated ore, network ore and disseminated ore.

(5) Ore deposits together with footwall mineralized zone and hanging-wall pelitic rock are considered to be dislocated by the tectonic movements.

(6) The results of drilling and electric logging show that pelitic rocks of the Küre Formation have extremely low resistivities. Basalt whose cracks and fractures caused by tectonic movements are filled by underground water, may show rather low resistivity.

(7) Drilling in this phase results in finding a mineralized zone at the northern extension of Zemberekler mineralized zone. The results of the survey indicate that the known ore deposits and mineralized zones are distributed in the N-S and NNW-SSE directions. The zones which are located in the N-S and NNW-SSE extensions from the mineralized zones in basalt with low resistivity anomalies, are promising for future exploration. Extremely low resistivity zones same as those in the known ore deposits are full of promise for finding of new ore deposits.

It is necessary to mind for deciding of drilling location that pelitic rocks show low resistivities, and it is difficult to distinguish ore deposits from pelitic rocks by resistivities.

1-2 Cünür Prospect

(1) The geology around the prospect is the Çangal meta-ophiolite consisting of pelitic schist, massive basalt, and green schist.

(2) The mineralized zone is composed of eight lenses and bedded gossans in green schist. The gossans consist of quartz-limonite-pyrite network and limonite dissemination in the silicified and argillized parts of mafic rocks.

(3) The results of time-domain IP survey show that resistivities of the zone extended below gossans are similar to those of the surrounding non-mineralized zone, and chargeabilities are lower than those of the surrounding silicified zones. The size of mineralized zones expected to occur below gossans is estimated to be small.

(4) Blind mineralized zones may not be expected below the extensively silicified zone which occurs around gossans, because chargeabilities of the zones below silicified zone are similar to those of surface outcrops.

(5) High chargeability anomalies are identified at the southern margin of the zone. These anomalies are located adjoining to the silicified zone. The shape on cross sections, chargeabilities, resistivities of these anomalies and geology suggest that these anomalies may indicate the existence of disseminated sulphide minerals.

1-3 Cozoğlu Prospect

(1) The geology around this prospect is composed mainly of the Çangal meta-ophiolite, the Kızacık Formation, and the Alaçam Formation. The meta-ophiolite consists of pelitic schist, massive metabasalt and green schist. The Kızacık Formation consists of grayish white limestone and the Alaçam Formation of quartz arenite and black mudstone.

(2) There are two openings of old adits, a large amount of slag and waste dumps on the surface. They are distributed in the Çangal meta-ophiolite.

(3) The mineralized zone observed in outcrops in this prospect is only a weak dissemination of pyrite.

(4) The results of geophysical survey in this phase show that high chargeability anomalies are distributed from the above zones which are covered by slags and waste dumps to the eastern part of this prospect. The shape of these anomalies on cross sections and the geology may indicate that bedded cupriferous pyrite deposits probably occur within these zones.

(5) The other high chargeability anomalies having similar values to the above mentioned anomalies are identified in the southern margin of the prospect, where is covered by the Çangal meta-ophiolite. It is considered that bedded cupriferous deposits may occur in these anomalous zones.

CHAPTER 2 RECOMMENDATIONS FOR THE THIRD PHASE SURVEY

Küre Zone

It is recommended that drilling exploration should be carried out in the following localities for the purpose of clarifying the conditions of subsurface copper mineralization in the third phase of the project.

- (1) South-southeast of the Aşıköy ore deposit
- (2) North-northwest of the Bakibaba ore deposit
- (3) East of the Bakibaba ore deposit and north-northwest of the Zemberekler mineralized zone

Cünür Prospect in the Taşköprü Zone

No further work is recommended in the Cünür prospect.

Cozoğlu Prospect in the Taşköprü Zone

It is recommended that drilling works should be carried out in the geophysical anomalies which are identified in the east of the localities where are occupied by slags for the purpose of clarifying the conditions of subsurface copper mineralization.

REFERENCE

REFERENCE

Geology

Balley, E.H., Barnes, J.W. and Kupfer, D.H. (1986): Geology and Ore Deposits of the Küre District, Kastamonu Province, Turkey.

Cas, R.A.F. (1992): Submarine Volcanism: Eruption Style, Products, and Relevance to Understanding the Host-Rock Successions to Volcanic-Hosted Massive Sulfide. *Mining Geology*, 87, 511-541

Çağtay, M.N. (1993): Hydrothermal alteration associated with volcanogenic massive sulfide deposits: Examples from Turkey, *Economic Geology*, 88, 606-621.

Etibank (1990): Küre ve Civarındaki Bakır Zuhurlarında Yapılan Çalışmalar Hakkında Rapor (unpublished in Turkish).

Ichige, Y., Furuno, M., Sakimoto, T. and Sowanaka, M. (1991): Exploration of the El Roble mine and its vicinity, Republic of Colombia, *Mining Geology*, 41, 77-93 (in Japanese).

Ichige, Y., Furuno, M., Hori, M. and Sowanaka, M. (1992): Application of stable isotope and minor elements analyses to the exploration of massive sulfide deposits.-An example in and around the El Roble mine, Republic of Colombia.-, *Mining Geology*, 42, 101-117 (in Japanese).

Iwasaki, M. (1972): Some problems on the ophiolite suite in relation to its lithologic sequence, special issue of *Mining Geology* (in Japanese).

Kosaka, H. and Kubota, Y. (1973): Lithogeochemical Study on the Diabase of the Shimokawa Mine, Hokkaido, *Mining Geology*, 23, 153-161 (in Japanese).

Kosaka, H. (1975): Geochemical Characteristics of the Shimokawa Diabase Sheets, Hokkaido, *Mining Geology*, 25, 161-174 (in Japanese).

Küre Bakırlı Pirit İşletmesi Müessesesi (1988), Etibank Bülteni, Sayı 112-113, Sa 47-57

Miyake, T. (1965): Texture of the ore Minerals from the Shimokawa Mine, *Mining Geology*, 15, 120-129 (in Japanese).

Miyake, T. (1965): On Spilitic Rocks of the Shimokawa Mine and their Genetical Relations to the Ore Deposits, *Mining Geology*, 15, 1-11 (in Japanese).

MTA (1962): Geology of the Sinop District, quadrangle series, scale 1:500,000.

Nielsen, H. (1979): Sulfur Isotopes, Lectures in Isotope Geology, Edited by E. Jäger and J.C. HUNZIKER, Springer-Verlag, p.283-312.

Sawkins, F.J. (1984): Metal Deposits in Relation to Plate Tectonics, Springer-Verlag, p.143-151.

Searle, D.L. (1972): Mode of occurrence of the cupriferous pyrite deposits of Cyprus. Inst. Mining Metallurgy Trans. 81, B189-B197

Takashima, K. (1977): Copper-Zinc-Lead Deposits of Turkey, Chishitu News, No.275, p.45-57 (in Japanese).

Ünsal, A. and Kafadar, S. (1990): Copper Exploration Project in the Vicinity of Küre-Taşköprü in Kastamonu (unpublished), Etibank.

Ünsal, A ve Dirim, M.S. (1990): Küre Civarındaki Bakır Zuhurlarında Yapılan Çalışmalar Hakkında Rapor, Etibank MAD Rap No.1445

Ünsal, A. (1991): Küre Bakırlı Pirit İşletmesi Sahalarında Yapılan Arama Çalışmaları ve Rezervlerine, ilişkin özet rapor

Yamagishi, H. (1987): Studies on the Neogene subaqueous lavas and hyaloclastites in Southwest Hokkaido. Rep.Geol.Surv.Hokkaido, 59, 55-117

Geophysical prospecting (IP Method)

Bertin, J. (1976): Experimental & Theoretical Aspect of IP. Vol.1. Presentation and Application of the IP Method Case Histories. Gebrüder Borntraeger, Berlin 1976, 250pp

Dey, A. and Morison, H.F. (1973): Electromagnetic Coupling in Frequency and Time domain Induced Polarization Surveys over Multilayered Earth. Geophysics. 38, 380-405.

Hohmann, G.W. (1973): Electromagnetic Coupling between Grounded Wires at the Surface of a Two Layered Earth. Geophysics, 38, 854-863

Keller, G.V. and Frischknecht, F.C. (1966): Electrical Methods in Geophysical Prospecting. Pergamon Press, London, 517pp

Madden, T.R., & T. Cantwell (1967): Induced Polarization. A Review, Mining Geophysics, 2, 373-400, S.E.G. Tulsa, Okla.

Parasnis, D.S. (1972): Principles of Applied Geophysics. Chapman & Hall, London.

Parasnis, D.S. (1973): Mining Geophysics. Elsevier, Amsterdam, 395pp

Pelton, W.H., Ward, S.H., Hallof, P.G., Sill, W.R., and Nelson, P.H. (1978) : Mineral Discrimination and Removal of Inductive Coupling with Multi-frequency IP. Geophysics, 43, 598-609

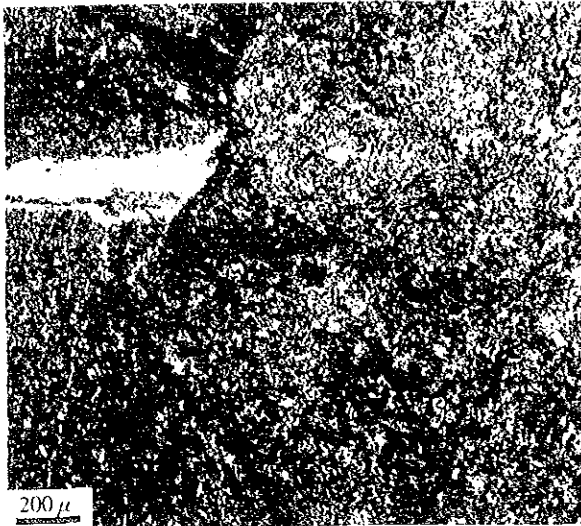
Sato, M. and Mooney, H.M. (1960): The Electrochemical Mechanism of Sulphide Self-potentials. Geophysics 25 No.1, pp226-249.

Scintrex Limited (1992): IPR-12 Time Domain IP/Resistivity Receiver operator Manual.

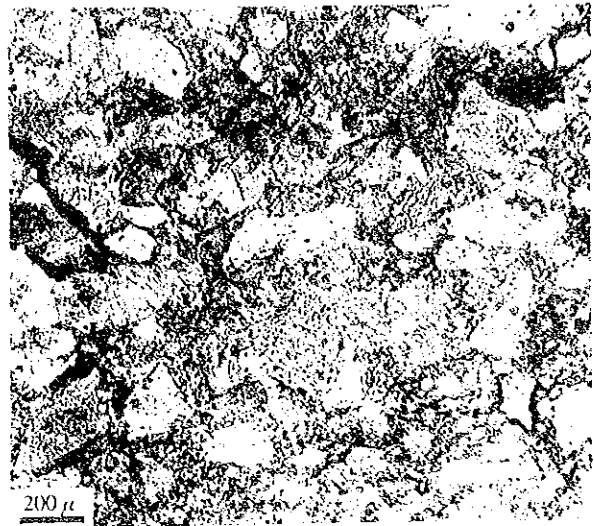
Seigel, H.O. (1959): Mathematical Formulation and Type Curves for Induced Polarization. Geophysics 24 547-565.

Seigel, H.O. (1967): The Induced Polarization Method. In L.W. Morley (Editor), Mining and Groundwater Geophysics. Geol. Rep., No. 26. Geol. Surv. Can. pp123-137.

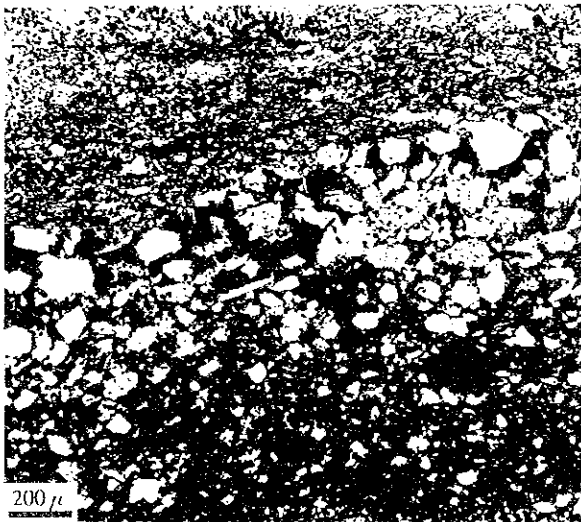
PHOTOGRAPHS



(Open Nicol)
Rock Name : Black Shale
Location : MJTK-1 378.0m



(Open Nicol)
Rock Name : Graywacke
Location : MJTK-4 30.5m

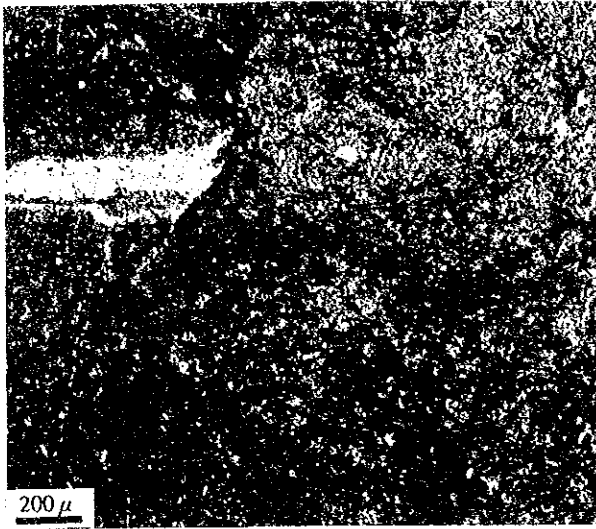


(Open Nicol)
Rock Name : Graywacke-Siltstone
Location : MJTK-1 139.7m

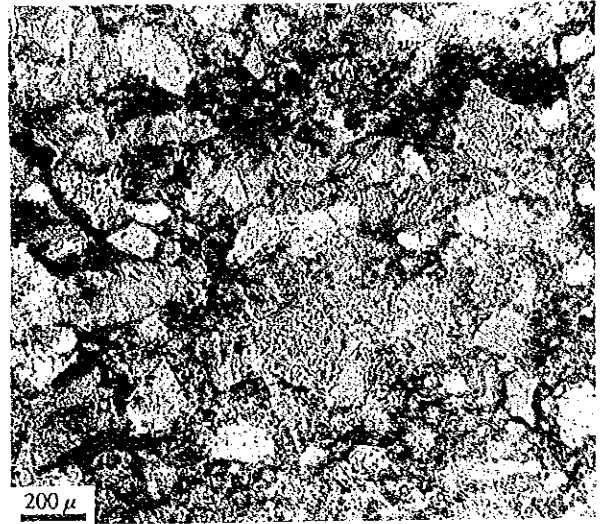


(Open Nicol)
Rock Name : Hyaloclastite
Location : MJTK-6 146.7m

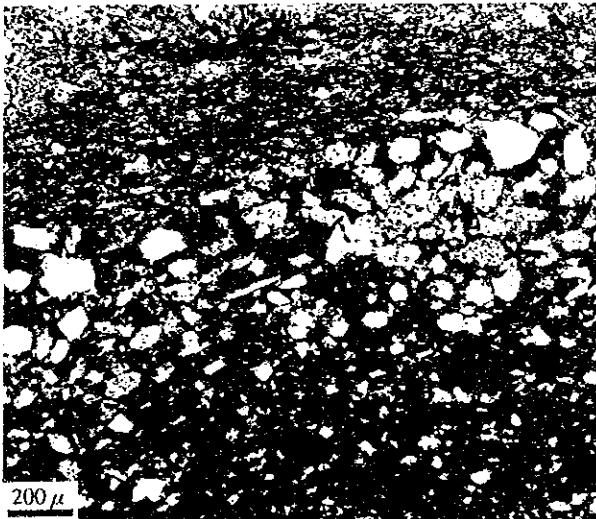
Photo. 1 Photomicrographs of Thin Sections



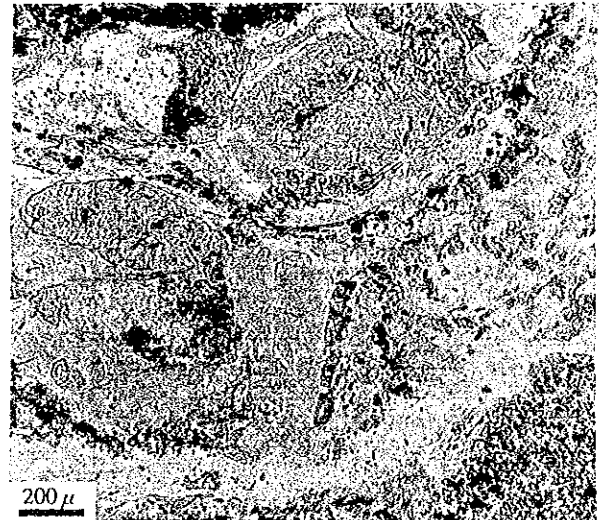
(Open Nicol)
Rock Name : Black Shale
Location : MJTK-1 378.0m



(Open Nicol)
Rock Name : Graywacke
Location : MJTK-4 30.5m

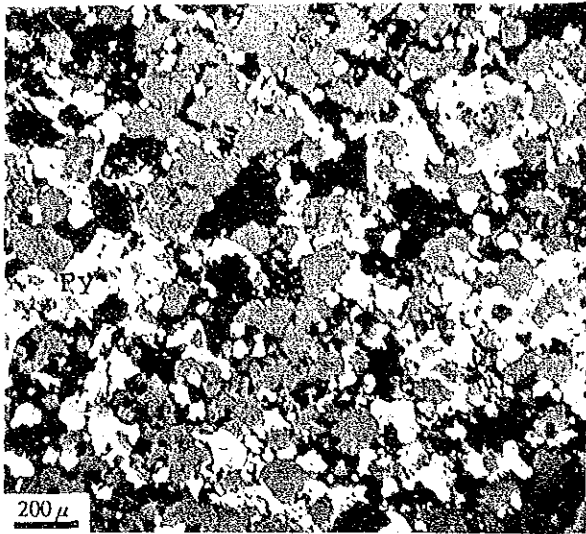


(Open Nicol)
Rock Name : Graywacke - Siltstone
Location : MJTK-1 139.7m

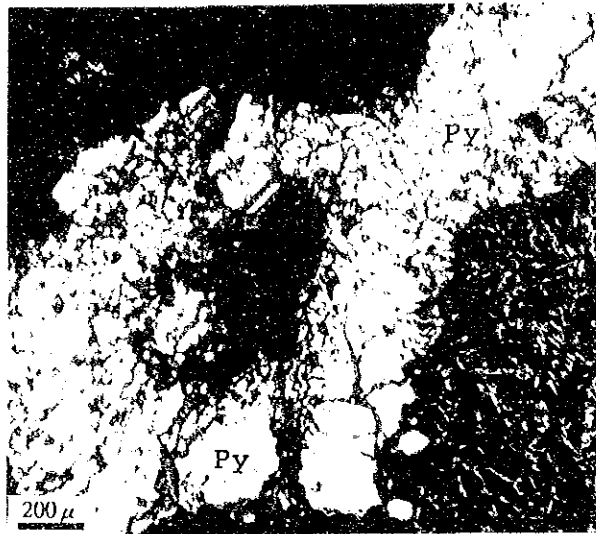


(Open Nicol)
Rock Name : Hyaloclastite
Location : MJTK-6 146.7m

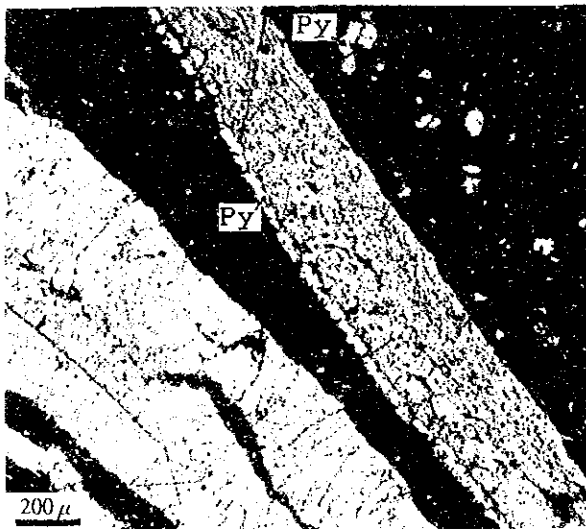
Photo. 1 Photomicrographs of Thin Sections



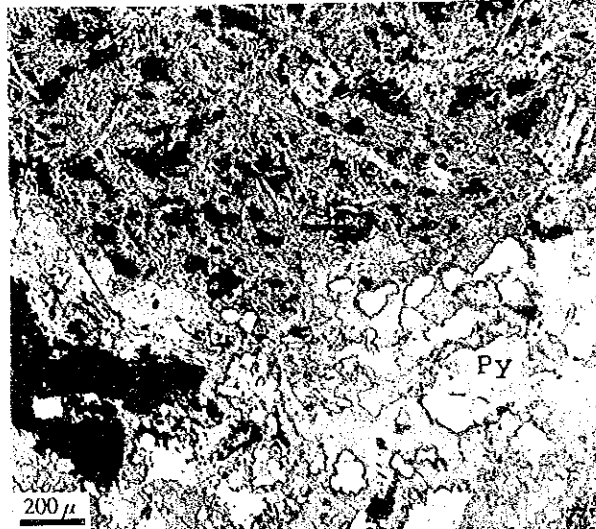
(Open Nicol)
 Sample Name : Pyrite Lens
 in Black Shale
 Location : MJTK-4 135.8m



(Open Nicol)
 Sample Name : Pyrite Film
 in Black Shale
 with Basalt Fragment
 Location : MJTK-4 182.8m



(Open Nicol)
 Sample Name : Calcite-
 Pyrite Veinlet and
 Pyrite Dissemination
 in Black Shale
 Location : MJTK-4 187.5m



(Open Nicol)
 Sample Name : Pyrite-Calcite Vein
 in Basalt
 Location : MJTK-4 198.0m

Photo. 2 Photomicrographs of Polished Sections

